Optical Spectroscopy of Superconducting $Ba_{0.55}K_{0.45}Fe_2As_2$: Evidence for Strong Coupling to Low-Energy Bosons

J. Yang,[1,2] D. Hüvonen,[3] U. Nagel,[3] T. Rõõm,[3] N. Ni,[4] P. C. Canfield,[4] S. L. Bud'ko,[4] J. P. Carbotte,[1,5] and T. Timusk[1,5,*]

[1]*Department of Physics and Astronomy, McMaster University, Hamilton, Ontario L8S 4M1, Canada*

[2]*Tianjin Key Laboratory of Composite and Functional Materials, School of Materials Science and Engineering, Tianjin University, Tianjin 300072, People's Republic of China*

[3]*National Institute of Chemical Physics and Biophysics, Akadeemia tee 23, 12618 Tallinn, Estonia*

[4]*Ames Laboratory and Department of Physics and Astronomy, Iowa State University, Ames, Iowa 50011, USA*

[5]*The Canadian Institute of Advanced Research, Toronto, Ontario M5G 1Z8, Canada*

(Received 7 July 2008; published 5 May 2009)

Normal state optical spectroscopy on single crystals of the new iron arsenide superconductor $Ba_{0.55}K_{0.45}Fe_2As_2$ shows that the infrared spectrum consists of two major components: a strong metallic Drude band and a well-separated midinfrared absorption centered at 0.7 eV. It is difficult to separate the two components unambiguously but several fits using Lorentzian peaks suggest a model with a Drude peak having a plasma frequency of 1.6 to 2.1 eV and a midinfrared peak with a plasma frequency of 2.5 eV. Detailed analysis of the frequency dependent scattering rate shows that the charge carriers interact with a broad bosonic spectrum extending beyond 100 meV with a very large coupling constant $\lambda = 3.4$ at low temperature. As the temperature increases this coupling weakens to $\lambda = 0.78$ at ambient temperature. This suggests a bosonic spectrum that is similar to what is seen in the lower T_c cuprates.

DOI: 10.1103/PhysRevLett.102.187003 PACS numbers: 74.25.Gz, 74.62.Dh, 74.72.Hs

With the discovery of superconductivity in the iron arsenic compounds with T_c's up to 54 K [1–8], an important question relates to the nature of the driving mechanism in this class of materials. For conventional superconductors the pairing glue is provided by the electron-phonon interaction and the energy gap has *s*-wave symmetry. Even MgB_2 with a $T_c = 40$ K falls in this same class but has the additional feature that two bands with distinct gap values are involved [9–11]. By contrast the gap in the cuprates has *d*-wave symmetry and there is a rapidly expanding body of evidence that the mechanism is the exchange of antiferromagnetic spin fluctuations [12–15]. Alternate explanations involving phonons have also been put forward [16,17].

Spectroscopic techniques have proven very useful in determining the physical mechanism of superconductivity. In the classic superconductors the spectroscopy of choice has been tunneling. Analysis of current-voltage data with an Eliashberg formalism has yielded a detailed picture of the electron-phonon spectral function $\alpha^2F(\Omega)$ [18,19], which agrees well with first principles calculations and also with similar data obtained from optics [20,21]. More recently similar information has been obtained about the electron-boson spectral density of the cuprates, mainly using infrared spectroscopy [22,23]. A complication that arises for this case is that even in the simplest approaches, the electron-boson spectral density involved can be different in the *d*- (pairing) and the *s*-wave (renormalization) channel which is a source of some uncertainty. Nevertheless, the preponderance of evidence is that this function involves the local spin susceptibility and points to a spin exchange mechanism. From this perspective the iron arsenic materials are particularly interesting. Recent density functional calculations have revealed low electron densities, a high density of states at the Fermi surface, and an attendant tendency towards itinerant magnetism [24–26]. At the same time calculations of $\alpha^2F(\Omega)$ have yielded a small value of the electron-phonon mass enhancement leading to doubt that these are electron-phonon superconductors [27]. Yet experiments indicate the gap has *s*-wave symmetry and involves several bands [28–30]. In view of these facts it is particularly important to see what light optical data can shed on the central question of pairing glue in the iron pnictide materials. With this goal in mind we focus on the normal state excitations just above T_c which are the source of superconductivity in boson exchange systems.

To extract the optical constants we used standard optical reflectance techniques over a wide range of frequencies ranging in photon energy from 5 meV to 5 eV at temperatures from 28 to 295 K [31]. The $Ba_{0.55}K_{0.45}Fe_2As_2$ single crystals were grown with a flux technique and had a nominal T_c of 28 K [8]. Figure 1 shows the measured reflectance on as-grown *ab* plane faces as a function of photon energy in meV at nine temperatures. At low energies the reflectance varies approximately linearly with frequency but there are features at 20 and 40 meV that get weaker as the temperature is raised. As a function of temperature there is a monotonic decrease of reflectance and there is a particularly rapid change in the reflectance at temperatures near 80 K. The inset shows the ambient temperature reflectance over a wider range of energies

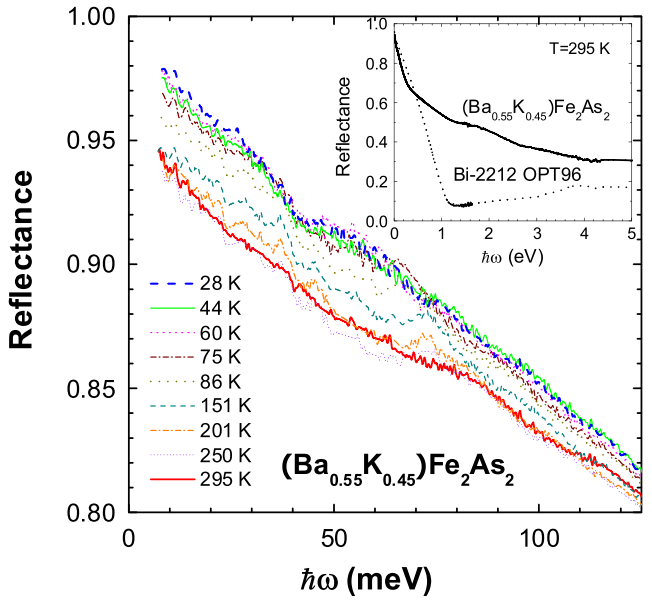

FIG. 1 (color online). The reflectance of $Ba_{1-x}K_xFe_2As_2$ as a function of incident photon energy at nine temperatures. The inset shows the reflectance at room temperature in a wider range of energies. There is a sharp break in the monotonic linear decay of reflectance at 0.5 eV signaling the presence of a strong midinfrared band. Also shown is the reflectance of a typical high temperature superconductor. The break at 0.5 eV is absent in this material and the strong linear decay of reflectance persists up to 1.2 eV.

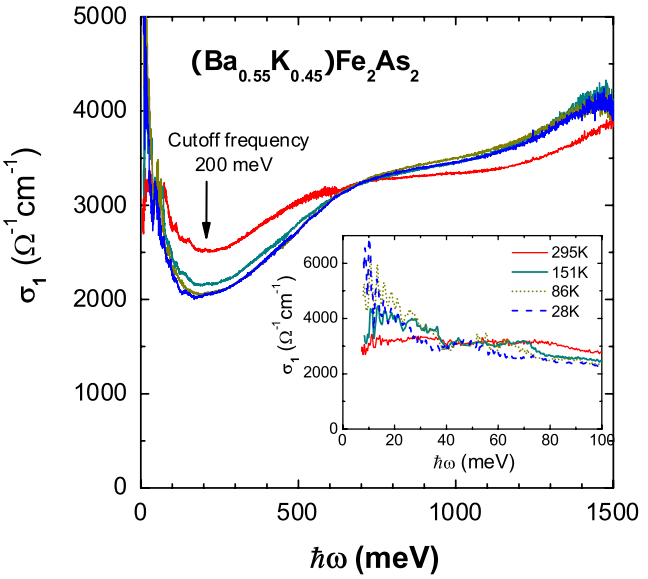

FIG. 2 (color online). The optical conductivity as a function of photon energy for four temperatures ordered from top 295 K to bottom 28 K at the position of the arrow. The inset shows the low frequency region on an expanded scale.

and a comparison with $Bi_2Sr_2CaCu_2O_{8+\delta}$ a familiar high temperature superconductor.

The measured reflectance was converted to an optical conductivity by Kramers-Kronig analysis. At low frequency Hagen-Rubens response was assumed and beyond 5 eV, free electron response was assumed. Figure 2 shows the optical conductivity at ambient temperature, at 28 K close to the superconducting transition temperature, and at two intermediate temperatures 86 and 151 K. We note a well-defined midinfrared peak at 0.7 eV and a separate Drude conductivity at low frequency, evidence of the metallic character of this material. As the temperature is lowered the Drude band narrows and there is a shift of spectral weight from the 200 meV region to above 1 eV, indicative of a rearrangement of electronic structure with temperature between 150 and 295 K. It is clear from Fig. 2 that it is difficult to separate the Drude band from the midinfrared band. Nevertheless, we have considered several models in which we have split the absorption into three components, the Drude and two finite frequency Lorentz oscillators. From these we obtain the plasma frequency of the Drude band to be in the range 1.8 to 2.1 eV. We also used an alternate model-independent method to estimate the plasma frequency, by integrating the measured conductivity without subtractions up to the minimum in conductivity at $\omega = 200$ meV (shown by an arrow in Fig. 2). The resulting analysis provides a value for the plasma frequency, $\omega_p = 1.6$ meV, that is comparable to that obtained using the oscillator fits. In the analysis that follows, we use this value for the plasma frequency.

To get information on the boson spectral density we apply an extended Drude model to the full conductivity to get the optical scattering rate of the charge carriers. This scattering rate is given by a generalized Drude formula

$$\sigma(T,\omega) = \frac{\Omega_p^2}{4\pi}\frac{1}{1/\tau(\omega) - i\omega(1+\lambda(\omega))}, \qquad (1)$$

where $\Omega_p^2 = 4\pi ne^2/m$ is the plasma frequency squared. The optical scattering rate $1/\tau(\omega) = \frac{ne^2}{m}\,\mathrm{Re}(1/\sigma(\omega))$ and the optical mass enhancement factor $\lambda(\omega)$ is given by $-\omega(1+\lambda(\omega)) = \frac{ne^2}{m}\,\mathrm{Im}(1/\sigma(\omega))$.

Figure 3 shows our results for the experimentally measured scattering rate $1/\tau(\omega)$ in the frequency range up to 100 meV at four temperatures in the normal state. In the frequency range below 100 meV, the midinfrared band does not contribute significantly to the conductivity, and hence the scattering rate can be extracted unambiguously in this frequency range. To get these results, a largely temperature independent broad feature between 40 and 60 meV in the conductivity was subtracted from the data. It is too sharp at 151 K to be part of the Drude absorption. Its spectral weight is small $\omega_p = 210$ meV and vanishes at room temperature suggesting that it is associated with a weak charge density modulation of the type seen in the cuprates [32].

From a knowledge of the optical scattering rate one can recover the underlying electron-boson spectral density

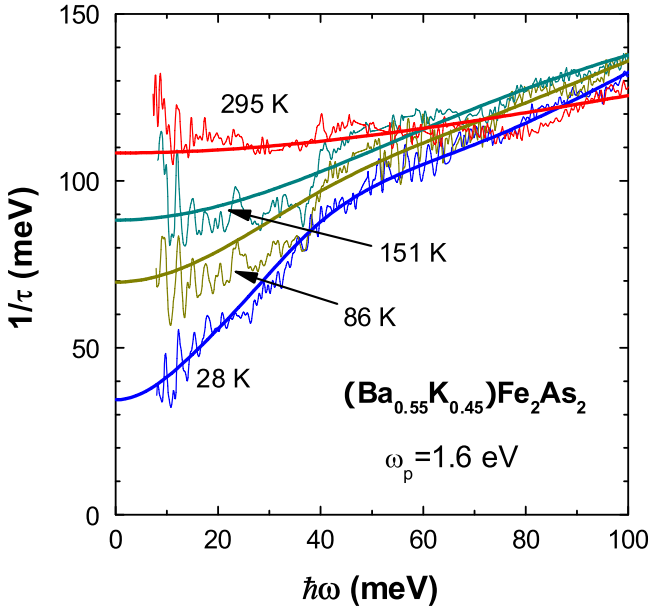

FIG. 3 (color online). Scattering rate $1/\tau(\omega)$ vs photon energy in the region below 140 meV at four temperatures (curves showing noise fluctuations) and maximum entropy calculations based on Eq. (2), using the bosonic functions shown in Fig. 4 (smooth curves).

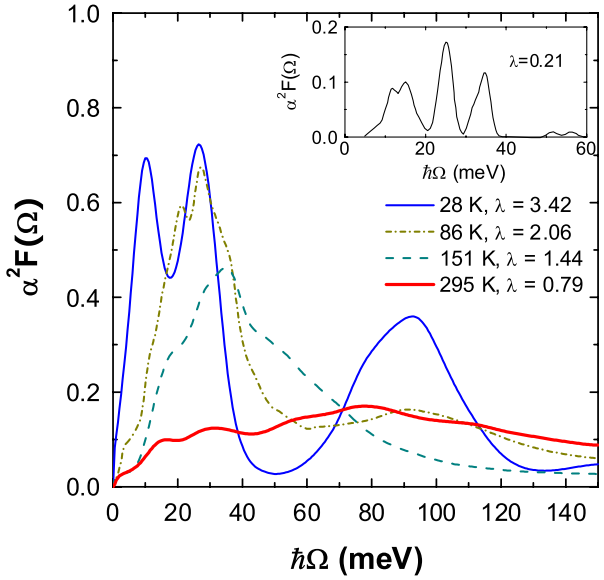

FIG. 4 (color online). Bosonic functions $\alpha^2F(\omega)$ extracted from the optical scattering rates of Fig. 3 using a maximum entropy inversion of Eq. (2). The inset is the calculated electron-phonon $\alpha^2F(\Omega)$ calculated by Boeri *et al.* with $\lambda = 0.21$.

$\alpha^2F(\Omega)$ through the inversion of the equation

$$1/\tau(\omega, T) = 1/\tau_{\text{imp}} + \int_0^\infty d\Omega K(\omega, \Omega, \Gamma)\alpha^2F(\Omega). \quad (2)$$

Here $1/\tau_{\text{imp}}$ is a residual elastic scattering rate due to impurities, and for the normal state at temperature T, the kernel $K(\omega, \Omega, T) = \frac{\pi}{\omega}[2\omega \coth(\Omega/2T) - (\omega + \Omega) \times \coth(\omega + \Omega/2T) + (\omega - \Omega)\coth(\omega - \Omega/2T)]$. The deconvolution of Eq. (2) through a maximum entropy technique is now standard [22,23,33]. The results are shown in Fig. 4 for the same four temperatures of Fig. 3. The residual scattering rate is 16.3 meV and the fits to the scattering rate are shown as the smooth solid curves in Fig. 3. A striking feature of our $\alpha^2F(\Omega)$ is its strong evolution with temperature from a three peak structure at low temperature towards a broad and featureless (incoherent) distribution of excitations at room temperature. At the lowest temperature $T = 28$ K just above T_c there is considerable spectral weight below ≈ 40 meV. While two peaks around 10 and 30 meV are resolved, they shift in energy and rapidly merge into a single feature as the temperature is increased. Such behavior is inconsistent with coupling to phonons even though the energies are in the right range as can seen in the inset of Fig. 4 where we reproduce the result of band structure calculations for the electron-phonon spectral density by Boeri *et al.* [27]. Their mass enhancement parameter is quite small, $\lambda = 0.21$, and cannot account for our results. We find a $\lambda = 3.42$ at $T = 28$ K which evolves to a value of 0.79 at ambient temperature as shown in Fig. 5. This behavior is very similar to what has been found for the cuprates where a temperature dependent bosonic spectrum is the norm. Similar spectra to those reported here have been observed both with neutron scattering [34,35] and optical spectroscopy [22,23] in the cuprates. Several theoretical models of spin fluctuations predict the formation of magnetic excitons as the temperature is lowered and a peak at low energy develops in the local susceptibility [36,37] as we see here below 40 meV. An angle resolved photoemission study in a closely related sample, $Ba_{0.6}K_{0.4}Fe_2As_2$ by Richard *et al.* [38], finds a mode at 13 meV which is connected to the antiferromagnetic wave

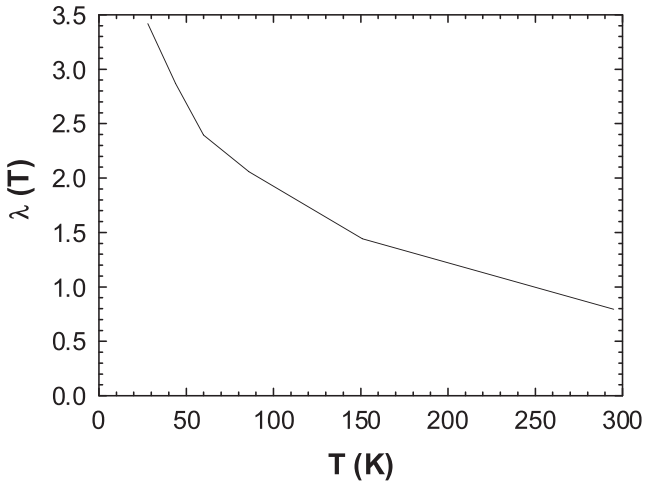

FIG. 5. The temperature dependence of the mass renormalization parameter $\lambda = 2\int d\Omega \alpha^2F(\Omega)/\Omega$ based on the $\alpha^2F(\Omega)$ of Fig. 4.

vector and has a strong temperature dependence which supports our findings.

An independent test of our bosonic model is the temperature dependence of the dc resistivity. There are several published dc resistivity curves [7,8,39] and they all show a curve that flattens substantially between low temperature and ambient temperature and are consistent with a temperature dependent λ. Further our own optical data can be analyzed in the low frequency limit to yield an optical resistivity. This is in good agreement with the data of Chen *et al.* [39]. The scattering rates in Fig. 3 are higher than the frequency, a characteristic of highly correlated systems.

In summary we find that optical spectroscopy data on crystals of $Ba_{0.55}K_{0.45}Fe_2As_2$ show that in addition to a midinfrared band this material has a substantial metallic Drude band. From the temperature and frequency dependence of this band we find that the charge carriers are coupled to a broad incoherent bosonic spectrum extending beyond 100 meV with a strongly temperature dependent coupling constant. This shows that these are not ordinary band metals. In the cuprates with $T_c = 90$ K, in the underdoped region, a resonance appears around 40 meV in the middle of a gap of the spin fluctuation spectrum at (π, π) in reciprocal space. Here we see a similar tendency of increasing spectral weight at 25 meV as the temperature is lowered. It remains to be seen if these parallel tendencies survive future experimental tests with better crystals and a wider range of compounds.

We thank E. Schachinger for the maximum entropy inversions shown in Fig. 4. This work has been supported by the Natural Science and Engineering Research Council of Canada and the Canadian Institute for Advanced Research. Sample growth and basic characterization done at the Ames Laboratory was supported by the Department of Energy, Basic Energy Sciences under Contract No. DE-AC02-07CH11358.

*timusk@mcmaster.ca.

[1] Y. Kamithara, T. Watanabe, M. Hirano, and H. Hosono, J. Am. Chem. Soc. **130**, 3296 (2008).
[2] H. Takahashi *et al.*, Nature (London) **453**, 376 (2008).
[3] G. F. Chen *et al.*, Phys. Rev. Lett. **100**, 247002 (2008).
[4] Z. A. Ren *et al.*, Chin. Phys. Lett. **25**, 2215 (2008).
[5] T. Y. Chen *et al.*, Nature (London) **453**, 1224 (2008).
[6] Y. Wang *et al.*, Supercond. Sci. Technol. **22**, 015018 (2009).
[7] M. Rotter, M. Tegel, and D. Johrendt, Phys. Rev. Lett. **101**, 107006 (2008).
[8] N. Ni, S. L. Budko, A. Kreyssig, S. Nandi, G. E. Rustan, A. I. Goldman, S. Gupta, J. D. Corbett, A. Kracher, and P. C. Canfield, Phys. Rev. B **78**, 014507 (2008).
[9] S. Tsuda *et al.*, Phys. Rev. Lett. **91**, 127001 (2003).
[10] N. Kristoffel, T. Örd, and K. Rägo, Europhys. Lett. **60**, 134 (2002).
[11] E. J. Nicol and J. P. Carbotte, Phys. Rev. B **71**, 054501 (2005).
[12] A. V. Chubukov *et al.*, in *The Physics of Superconductors*, edited by K. H. Bennemann and J. B. Ketterson (Springer, Berlin, 2003), Vol. II, pp. 495–590.
[13] J. P. Carbotte, E. Schachinger, and D. N. Basov, Nature (London) **401**, 354 (1999).
[14] Ar. Abanov and A. V. Chubukov, Phys. Rev. Lett. **83**, 1652 (1999).
[15] J. F. Zasadzinski *et al.*, Phys. Rev. Lett. **96**, 017004 (2006).
[16] T. Cuk *et al.*, Phys. Rev. Lett. **93**, 117003 (2004).
[17] X. J. Zhou *et al.*, Phys. Rev. Lett. **95**, 117001 (2005).
[18] W. L. McMillan and J. M. Rowell, Phys. Rev. Lett. **14**, 108 (1965).
[19] J. P. Carbotte, Rev. Mod. Phys. **62**, 1027 (1990).
[20] B. Farnworth and T. Timusk, Phys. Rev. B **14**, 5119 (1976).
[21] N. Bock and D. Coffey, Phys. Rev. B **76**, 174513 (2007).
[22] J. Hwang, T. Timusk, E. Schachinger, and J. P. Carbotte, Phys. Rev. B **75**, 144508 (2007).
[23] J. Hwang, E. Schachinger, J. P. Carbotte, F. Gao, D. B. Tanner, and T. Timusk, Phys. Rev. Lett. **100**, 137005 (2008).
[24] D. J. Singh and M. H. Du, Phys. Rev. Lett. **100**, 237003 (2008).
[25] C. de la Cruz *et al.*, Nature (London) **453**, 899 (2008).
[26] I. I. Mazin *et al.*, Phys. Rev. Lett. **101**, 057003 (2008).
[27] L. Boeri, O. V. Dolgov, and A. A. Golubov, Phys. Rev. Lett. **101**, 026403 (2008).
[28] G. Liu *et al.*, Phys. Rev. Lett. **101**, 177005 (2008).
[29] L. Zhao *et al.*, Chin. Phys. Lett. **25**, 4402 (2008).
[30] H. Ding *et al.*, Europhys. Lett. **83**, 47001 (2008).
[31] C. C. Homes, M. A. Reedyk, D. A. Crandles, and T. Timusk, Appl. Opt. **32**, 2976 (1993).
[32] J. Hwang, J. Yang, T. Timusk, S. G. Sharapov, J. P. Carbotte, D. A. Bonn, R. Liang, and W. N. Hardy, Phys. Rev. B **73**, 014508 (2006).
[33] E. Schachinger, D. Neuber, and J. P. Carbotte, Phys. Rev. B **73**, 184507 (2006).
[34] C. Stock, W. J. L. Buyers, R. A. Cowley, P. S. Clegg, R. Coldea, C. D. Frost, R. Liang, D. Peets, D. Bonn, W. N. Hardy, and R. J. Birgeneau, Phys. Rev. B **71**, 024522 (2005).
[35] B. Vignolle, S. M. Hayden, D. F. McMorrow, H. M. Rønnow, B. Lake, C. D. Frost, and T. G. Perring, Nature Phys. **3**, 163 (2007).
[36] Ar. Abanov and A. V. Chubukov, Phys. Rev. Lett. **83**, 1652 (1999).
[37] P. Prelovšek and I. Sega, Phys. Rev. B **74**, 214501 (2006)
[38] P. Richard *et al.*, Phys. Rev. Lett. **102**, 047003 (2009).
[39] G. F. Chen *et al.*, Phys. Rev. B **78**, 224512 (2008).